

The spectral changes for the solution of Ni(Me₄daes)-Br₂ in *o*-dichlorobenzene, from room temperature to 170°, are shown in Figure 3. The new bands at 14,900 and 16,700 cm⁻¹ for the cobalt complex and at 9300, 10,700, and 19,300 cm⁻¹ for the nickel complex are characteristic of distorted tetrahedral species of these two elements. In fact, these bands are also shown by tetrahedral ML₂X₂ complexes, where M = Co, Ni; L = (CH₃)₂N(CH₂)_nN(CH₃)₂, with *n* = 2, 3; X = Cl, Br.¹⁹ In the solutions of the Ma₄daes complexes there

are, therefore, also distorted tetrahedral species, the percentage of which increases with increasing temperature.

Acknowledgment.—Thanks are expressed to Professor L. Sacconi for helpful discussions. We are indebted to Dr. N. Nardi for experimental assistance. The financial support of the Italian "Consiglio Nazionale delle Ricerche" is gratefully acknowledged.

(19) L. Sacconi, I. Bertini, and F. Mani, *Inorg. Chem.*, **6**, 262 (1967).

CONTRIBUTION FROM THE DEPARTMENT OF CHEMISTRY,
COLUMBIA UNIVERSITY, NEW YORK, NEW YORK 10027

The Crystal and Molecular Structure of an Oxo-Bridged Binuclear Iron(III) Complex, [(HEDTA)FeOFe(HEDTA)]²⁻

By STEPHEN J. LIPPARD, HARVEY SCHUGAR, AND CHEVES WALLING

Received April 3, 1967

The crystal and molecular structure of ethylenediammonium N-hydroxyethylethylenediaminetriacetatoiron(III)-*μ*-oxo-N-hydroxyethylethylenediaminetriacetatoferrate(III) hexahydrate, (enH₂)[(HEDTA)FeOFe(HEDTA)]·6H₂O, has been determined by a three-dimensional X-ray crystallographic analysis. The compound crystallizes as bright red prisms in space group P2₁/c with unit cell dimensions *a* = 18.22, *b* = 11.50, *c* = 17.42 Å, β = 103° 55', and *Z* (for the dimer) = 4. From approximately 2350 independent nonzero reflections estimated visually from Weissenberg photographs, the structure was solved by the use of conventional Patterson, Fourier, and least-squares refinement techniques to a final value for the discrepancy index, *R*, of 0.114. The geometry of the anion consists of two Fe(HEDTA) moieties in which the HEDTA ligand is pentadentate. These are connected by an approximately linear oxo bridge (Fe–O–Fe = 165.0°), having relatively short Fe–O distances of 1.79 Å. A qualitative molecular orbital description of the complex is presented.

Introduction

Recent studies of the spectral and magnetic properties of Fe(III)–EDTA, Fe(III)–HEDTA, and other related iron(III) systems, both in aqueous solution and in the solid state, have been interpreted in terms of a monomer–dimer equilibrium.^{1,2} Among the compounds investigated was a low-spin Fe(III)–HEDTA complex which, primarily on the basis of its infrared spectrum and magnetic moment, was assigned the structure [(HEDTA)Fe–O–Fe(HEDTA)]²⁻, where the HEDTA groups were thought to be pentadentate. Although linear metal–oxygen–metal groups have been proposed frequently in the past to account for certain properties of first-row transition metal complexes,³ few have been structurally characterized by X-ray diffraction.^{4–7} It was therefore of interest to us to

determine the X-ray structure of the crystalline compound (enH₂)[(HEDTA)FeOFe(HEDTA)]·6H₂O reported earlier.^{1,2} The results, which are presented here, fully corroborate the previous structural assignment and, in addition, provide new information concerning the nature of the bonding in this and related complexes containing linear M–O–M groupings.

Experimental Procedures and Results

Collection and Reduction of X-Ray Data.—The compound was prepared as described previously¹ and recrystallized from a hot dimethylformamide–water solution. The crystal used in all X-ray studies reported here was a small red prism having a mean cross section of 0.1 mm. Airplane glue was used to mount the crystal on the end of a glass fiber along the *b* axis. After an approximate optical alignment, the crystal was transferred to the precession camera where the space group and unit cell dimensions were determined using Zr-filtered Mo Kα radiation (λ 0.7107 Å). The density was measured by flotation in a mixture of carbon tetrachloride and chloroform.

Intensity data were collected on the Weissenberg camera using molybdenum radiation filtered through zirconium. With this radiation, the linear absorption coefficient μ was calculated to be 9.47 cm⁻¹, resulting in a value of 0.047 for μR_{max}. Since the maximum effect of absorption on the intensities was estimated to be less than 2%, no absorption corrections were applied. The intensities of approximately 2350 nonzero reflections, for which

(1) H. Schugar, C. Walling, R. B. Jones, and H. B. Gray, *J. Am. Chem. Soc.*, **89**, 3712 (1967).

(2) EDTA = ethylenediaminetetraacetate; HEDTA = N-hydroxyethylethylenediaminetriacetate; enH₂⁺ = ethylenediammonium cation.

(3) Examples include: (a) titanium: K. Watenpaugh and C. N. Cauglan, *Inorg. Chem.*, **6**, 963 (1967); (b) vanadium: T. W. Newton and F. B. Baker, *ibid.*, **3**, 569 (1964); (c) chromium: A. Earnshaw and J. Lewis, *J. Chem. Soc.*, 396 (1961); (d) manganese: L. H. Vogt, A. Zalkin, and D. H. Templeton, *Science*, **151**, 569 (1966); (e) iron: G. Anderegg, *Helv. Chim. Acta*, **45**, 1643 (1962), and ref 1 and 3b.

(4) Cf. ref 3a and 3d. Also, note the recent communication by E. Fleischer and J. Hawkinson, *J. Am. Chem. Soc.*, **89**, 721 (1967), which reports the structure of a seven-coordinate Fe(III) dimer containing macrocyclic, polydentate ligands.

(5) Several structural studies of second- and third-row transition metal complexes containing M–O–M groups have been carried out, e.g., [Cl₅RuORuCl₅]⁴⁻ and [Cl₅ReOReCl₅]²⁻.

(6) A. M. Matheson, D. P. Mellor, and N. C. Stephenson, *Acta Cryst.*, **5**, 185 (1952).

(7) J. C. Morrow, *ibid.*, **15**, 851 (1962).

$(\sin \theta)/\lambda \leq 0.527$, were obtained from equiinclination Weissenberg photographs $h0l-h11l$ using the multiple-film technique. Each spot was compared with a scale prepared from timed exposures of one reflection from the same crystal.

The raw data, I , were corrected for the usual Lorentz-polarization effects and then placed on an approximate common scale through a modification of Wilson's method.⁸ From the resultant values for $|F_o|$ and $|F_o|^2$, the structure was solved by the usual Patterson, Fourier, and least-squares refinement processes (*vide infra*). Scattering factors for the zerovalent atoms were obtained from the "International Tables."⁹ Anomalous dispersion effects are small¹⁰ in the present case, and, consequently, no corrections were applied. Weights were assigned to each reflection in the least-squares process according to the following scheme: $\sigma = 5/I$ for $I \leq 5$; $\sigma = I/180$ for $I \geq 180$; $\sigma = 1.0$ for $5 < I < 180$, where the weights w were taken as $1/\sigma^2$.

Unit Cell and Space Group.—The complex $(enH_2)[(HEDTA)FeOFe(HEDTA)] \cdot 6H_2O$ crystallizes in the monoclinic system with $a = 18.22 \pm 0.02$, $b = 11.50 \pm 0.01$, $c = 17.42 \pm 0.02$ Å, and $\beta = 103^\circ 55'$. The cell volume ($V = 3543$ Å³) and density ($\rho = 1.584 \pm 0.004$ g/cc) require four dimeric formula weights per unit cell. The calculated density, 1.590 g/cc, agrees well with that observed. From the observed extinctions $h0l$, $l \neq 2n$, and $0k0$, $k \neq 2n$, the space group was ascertained to be $P2_1/c$.¹¹ All atoms occupy the general fourfold set of positions (4c): $\pm(x, y, z)$ and $\pm(x, 1/2 - y, 1/2 + z)$.

Determination of the Structure.—Using the corrected data, an origin-removed, sharpened Patterson map was computed and solved for the positions of the two crystallographically independent iron atoms.⁸ A difference Fourier synthesis was then performed with the signs of the structure factors assigned on the basis of the trial positional parameters for the iron atoms. From the Fourier map, several light-atom peaks were located and used along with the iron atoms (after a cycle of least-squares refinement) to phase a second difference map. Subsequent cycles of least-squares refinement, structure factor calculation, and Fourier synthesis revealed the positions of all 51 nonhydrogen atoms in the asymmetric unit. Five such cycles were necessary, after which the discrepancy factors $R_1 = \Sigma||F_o| - |F_c||/\Sigma|F_o|$ and $R_2 = (\Sigma w(|F_o| - |F_c|)^2/\Sigma w F_o^2)^{1/2}$ were 0.154 and 0.166, respectively. Further refinements of first positional parameters and then the scale factors and isotropic thermal parameters¹² were carried out until the variation in each parameter was less than one-third the value of its standard deviation. The final values for the discrepancy factors were $R_1 = 0.114$ and $R_2 = 0.117$. A final difference Fourier map revealed no peaks having electron density greater than 0.94 e/Å³ and showed no evidence of anisotropic thermal motion in the iron atoms, at which point the structure was considered to have been completed.

Table I contains the final list of calculated and observed structure factors. The atomic positional and isotropic temperature parameters, along with their standard deviations as derived from the inverse matrix of the final least-squares refinement cycle, are given in Table II.

Discussion of the Structure

Packing Considerations.—The crystal structure of $(enH_2)[(HEDTA)FeOFe(HEDTA)] \cdot 6H_2O$ consists of discrete ethylenediammonium cations and binuclear, oxo-bridged anions (Figure 1). Each cation is associ-

(8) Programs for the IBM 7094 used in this work include local versions of the Zalkin Fourier program **FORDAP**, the Busing-Martin-Levy structure factor calculation and least-squares refinement program, **OR-FLS**, the Busing-Martin-Levy error function program, **OR-FFE**, the molecular geometry program, **MGEOM**, written by Dr. J. S. Wood, as well as various other data reduction programs kindly made available to us through the courtesy of the Brookhaven National Laboratories.

(9) "International Tables for X-Ray Crystallography," Vol. III, The Kynoch Press, Birmingham, England, 1962, pp 202, 210.

(10) See ref 9, p 215.

(11) See ref 9, Vol. I, p 99.

(12) It was not possible for us to refine all parameters simultaneously owing to insufficient core storage space in our IBM 7094 computer.

TABLE II

FINAL POSITIONAL PARAMETERS AND ISOTROPIC TEMPERATURE FACTORS FOR $(enH_2)[(HEDTA)FeOFe(HEDTA)] \cdot 6H_2O$ ^{a,b}

Atom	x	y	z	B, Å ²
FeA	0.3457 (1)	0.0963 (2)	0.2728 (2)	2.31 (6)
FeB	0.1456 (1)	0.1192 (2)	0.2343 (2)	2.22 (6)
OXO	0.2444 (7)	0.0882 (9)	0.2570 (8)	3.4 (2)
O1A	0.3291 (8)	0.3232 (11)	0.0729 (8)	4.1 (3)
O2A	0.3545 (7)	0.2550 (10)	0.2225 (7)	3.1 (2)
O3A	0.3477 (7)	0.4446 (10)	0.2374 (8)	4.0 (3)
O4A	-0.4408 (9)	0.4774 (14)	0.4014 (10)	5.9 (4)
O5A	-0.3610 (8)	0.5131 (11)	0.3252 (8)	4.2 (3)
O6A	-0.3702 (6)	0.4553 (9)	0.1584 (7)	2.7 (2)
O7A	-0.4527 (8)	0.3172 (11)	0.1067 (8)	4.6 (3)
O1B	0.1869 (7)	0.3494 (11)	0.4344 (8)	4.0 (3)
O2B	0.1460 (7)	0.2859 (10)	0.2729 (8)	3.4 (3)
O3B	0.1646 (7)	0.4730 (10)	0.2467 (8)	3.8 (3)
O4B	0.0269 (8)	0.0417 (11)	0.3970 (9)	4.5 (3)
O5B	0.1150 (7)	0.0566 (10)	0.3320 (7)	3.4 (2)
O6B	-0.1174 (7)	0.4749 (9)	0.3308 (7)	2.8 (2)
O7B	-0.0268 (8)	0.3667 (12)	0.4053 (8)	4.9 (3)
OW1	-0.1733 (8)	0.4069 (12)	0.0394 (8)	4.9 (3)
OW2	-0.2348 (7)	0.3698 (11)	0.3838 (8)	4.3 (3)
OW3	-0.1878 (9)	0.1021 (14)	0.0508 (9)	6.2 (4)
OW4	-0.3823 (12)	0.1135 (21)	0.0458 (13)	9.9 (5)
OW5	-0.0998 (8)	0.1615 (12)	0.4254 (9)	5.1 (3)
OW6	-0.3136 (8)	0.0606 (12)	0.4297 (9)	5.1 (3)
N1A	0.3793 (9)	0.2100 (12)	0.3773 (9)	2.9 (3)
N2A	0.4735 (8)	0.0913 (12)	0.2915 (9)	2.8 (3)
N1B	0.1270 (8)	0.2221 (11)	0.1207 (9)	2.6 (3)
N2B	0.0183 (8)	0.1351 (12)	0.2015 (9)	3.0 (3)
N3	-0.2474 (9)	0.1454 (13)	0.3104 (9)	3.7 (3)
N4	-0.2749 (11)	0.2820 (17)	0.1074 (12)	5.7 (4)
C1A	0.3620 (11)	0.2427 (17)	0.5189 (13)	3.9 (4)
C2A	0.3419 (11)	0.1701 (15)	0.4421 (12)	3.2 (4)
C3A	0.3557 (11)	0.3295 (15)	0.3523 (12)	3.3 (4)
C4A	0.3532 (10)	0.3461 (13)	0.2675 (11)	2.6 (4)
C5A	0.4654 (11)	0.2054 (16)	0.4085 (12)	3.2 (4)
C6A	0.5039 (11)	0.1942 (15)	0.3420 (11)	3.1 (4)
C7A	0.4863 (11)	0.0937 (16)	0.2127 (12)	3.5 (4)
C8A	0.4267 (13)	0.0207 (18)	0.1590 (13)	4.2 (5)
C9A	0.4990 (10)	-0.0204 (15)	0.3340 (11)	3.0 (4)
C10A	-0.4361 (10)	0.4088 (15)	0.1397 (11)	3.1 (4)
C1B	0.1525 (11)	0.2739 (14)	0.4833 (12)	3.1 (4)
C2B	0.1652 (11)	0.1632 (15)	0.0627 (12)	3.2 (4)
C3B	0.1596 (10)	0.3386 (14)	0.1447 (11)	2.7 (4)
C4B	0.1550 (9)	0.3696 (13)	0.2278 (11)	2.6 (3)
C5B	0.0424 (11)	0.2314 (16)	0.0817 (12)	3.4 (4)
C6B	-0.0021 (11)	0.2347 (15)	0.1477 (12)	3.3 (4)
C7B	-0.0052 (11)	0.1487 (16)	0.2766 (11)	3.3 (4)
C8B	0.0474 (12)	0.0791 (17)	0.3394 (13)	4.1 (4)
C9B	-0.0124 (11)	0.0238 (15)	0.1613 (12)	3.4 (4)
C10B	-0.0474 (11)	0.4474 (15)	0.3610 (12)	3.2 (4)
C1C	-0.2340 (12)	0.2513 (18)	0.1902 (13)	4.4 (4)
C2C	-0.2919 (12)	0.1883 (18)	0.2319 (13)	4.3 (4)

^a Standard deviations, in parentheses beside each entry, occur in the last significant figure for each parameter. ^b The atom-labeling system used refers to that of Figure 2.

ated with several water molecules *via* hydrogen-bonded interactions. Similarly, the N-hydroxyethyl and several carboxylate groups of the anion are hydrogen-bonded to lattice water molecules. The more important hydrogen-bonded contact distances (<3.0 Å) are summarized in Table III. It is evident that the lattice water molecules play an important role in cementing the structure together. Apart from hydrogen-bonded interactions, no other significant interactions occur in the crystal structure of $(enH_2)[(HED-$

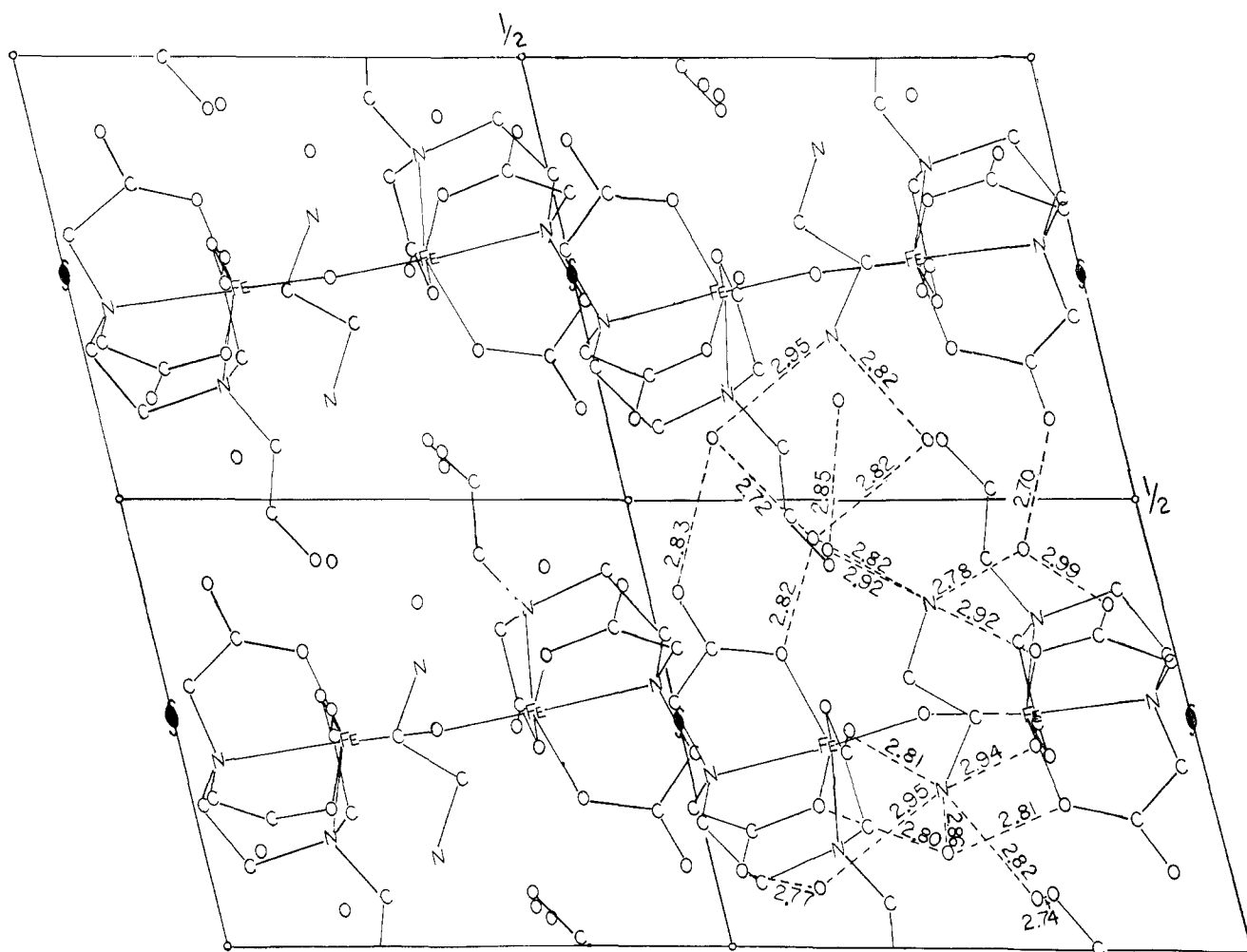


Figure 1.—The crystal structure of $(\text{enH}_2)[(\text{HEDTA})\text{FeOFe}(\text{HEDTA})] \cdot 6\text{H}_2\text{O}$ in the (010) projection. Direct bonding is indicated by solid lines, and close nonbonded contacts ($<3.0 \text{ \AA}$) by dashed lines (see Table III for the identification of hydrogen-bonded interactions). The origin is taken at the center of the diagram, with a horizontal and c approximately vertical.

TABLE III
HYDROGEN-BONDED CONTACT DISTANCES ($<3.0 \text{ \AA}$) IN THE
CRYSTAL STRUCTURE OF
 $(\text{enH}_2)[(\text{HEDTA})\text{FeOFe}(\text{HEDTA})] \cdot 6\text{H}_2\text{O}^a$

Atoms hydrogen-bonded ^b		
Hydrogen donor	Acceptor	Distance, \AA^c
N3	OW2	2.86 (3)
N3	OW5	2.95 (2)
N3	OW6	2.82 (2)
N4	OW1	2.82 (2)
N4	OW3	2.92 (3)
N4	OW4	2.78 (3)
OW1	OW5	2.72 (2)
OW1	O5B	2.82 (2)
OW2	O5A	2.81 (2)
OW2	O6B	2.80 (2)
OW3	OW2	2.85 (2)
OW4	O4A	2.70 (3)
OW4	O7A	2.99 (3)
OW5	O4B	2.83 (2)
OW5	O7B	2.77 (2)
OW6	OW1	2.82 (2)
O1A	OW6	2.74 (2)
O1B	OW3	2.92 (2)

^a See Table II and Figure 2 for atom-labeling scheme. ^b Identification of hydrogen-donor and -acceptor atoms was made on the basis of a careful examination of a three-dimensional model. ^c Numbers in parentheses are estimated standard deviations.

$(\text{enH}_2)[(\text{HEDTA})\text{FeOFe}(\text{HEDTA})] \cdot 6\text{H}_2\text{O}$, the distances between individual, nonbonded atoms all being equal to or greater than the sum of their van der Waals radii. Further details may be obtained from Figure 1 which displays the crystal packing relations in the (010) projection.

The Binuclear $[(\text{HEDTA})\text{FeOFe}(\text{HEDTA})]^{2-}$ Anion.—A somewhat idealized drawing of the binuclear anion showing the atom-labeling scheme appears in Figure 2. Although the complex has no crystallographically required symmetry, it is evident from Tables IV–VI that corresponding dimensions in the two halves of the molecule are all identical within the limits of significance (± 3 esd). In fact, the dimer comes close to having a C_2 axis through the bridging oxygen atom (Figure 2).

Table IV summarizes the geometry of the inner coordination group, *i.e.*, all distances and angles for bonds to the iron atoms. The general structure can be described roughly as consisting of two distorted octahedra sharing an oxygen atom so as to form an approximately linear Fe–O–Fe group. The deviation from linearity ($\text{Fe–O–Fe} = 165.0 \pm 0.8^\circ$) is significant.

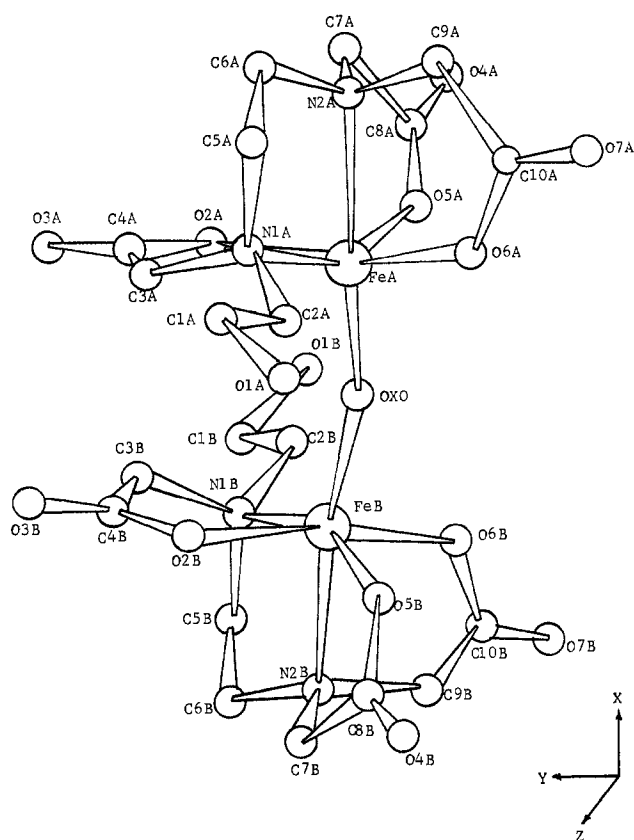


Figure 2.—Slightly idealized perspective drawing of the $[(\text{HEDTA})\text{FeOFe}(\text{HEDTA})]^{2-}$ anion showing the atom-labeling scheme. In the cation, the atoms were labeled N3—C2C—C1C—N4. The six lattice water oxygen atoms were labeled OW1, OW2, ..., OW6.

TABLE IV

GEOMETRY OF THE INNER COORDINATION GROUP:
BOND LENGTHS AND ANGLES ABOUT THE IRON ATOMS^{a,b}

Bond length	Distance, A	Bond length	Distance, A
FeA—OXO	1.80 (1)	FeB—OXO	1.79 (1)
FeA—N1A	2.20 (1)	FeB—N1B	2.26 (1)
FeA—N2A	2.27 (1)	FeB—N2B	2.26 (1)
FeA—O2A	2.05 (1)	FeB—O2B	2.03 (1)
FeA—O5A	2.03 (1)	FeB—O5B	2.05 (1)
FeA—O6A	2.00 (1)	FeB—O6B	2.01 (1)
Interbond angle	Angle, deg	Interbond angle	Angle, deg
FeA—OXO—FeB	165.0 (8)	OXO—FeB—N1B	103.5 (6)
OXO—FeA—N1A	103.3 (6)	OXO—FeB—N2B	172.9 (6)
OXO—FeA—N2A	175.5 (5)	OXO—FeB—O2B	101.1 (6)
OXO—FeA—O2A	99.3 (6)	OXO—FeB—O5B	102.0 (5)
OXO—FeA—O5A	100.8 (6)	OXO—FeB—O6B	93.8 (5)
OXO—Fe—O6A	97.1 (5)	O2B—FeB—O5B	92.1 (5)
O2A—FeA—O5A	91.1 (5)	O2B—FeB—O6B	161.5 (5)
O2A—FeA—O6A	161.7 (5)	O2B—FeB—N1B	77.5 (5)
O2A—FeA—N1A	77.9 (5)	O2B—FeB—N2B	86.0 (5)
O2A—FeA—N2A	84.3 (5)	O5B—FeB—O6B	95.5 (5)
O5A—FeA—O6A	93.8 (5)	O5B—FeB—N1B	154.1 (5)
O5A—FeA—N1A	154.9 (6)	O5B—FeB—N2B	76.7 (5)
O5A—FeA—N2A	76.5 (5)	O6B—FeB—N1B	88.5 (5)
O6A—FeA—N1A	90.5 (5)	O6B—FeB—N2B	79.4 (5)
O6A—FeA—N2A	79.7 (5)	N1B—FeB—N2B	78.9 (5)
N1A—FeA—N2A	80.0 (5)		

^a See Figure 2 for atom-labeling scheme. ^b Numbers in parentheses are estimated standard deviations.

TABLE V

EQUATIONS OF MOLECULAR PLANES PERPENDICULAR TO THE Fe—O—Fe AXIS AND DISTANCES OF ATOMS IN ANGSTROMS FROM THESE PLANES^{a,b}

Plane through O2A, N1A, O5A, O6A
 $1.011X + 54.65Y + 6.988Z = 6.142$

O2A	-0.08 (3)	O5A	0.07 (3)
N1A	0.09 (3)	O6A	-0.07 (3)
FeA	-0.36 (1)		

Plane through O2B, N1B, O5B, O6B
 $1.040X - 7.519Y + 4.191Z = 2.013$

O2B	0.11 (4)	O5B	-0.08 (3)
N1B	-0.13 (4)	O6B	0.08 (3)
FeB	0.36 (1)		

^a See Figure 2 for atom-labeling scheme. ^b Weighted least-squares planes were calculated with reference to an orthogonal coordinate system in which the Y axis is taken to be coincident with the cell *b* axis, the Z axis is in the direction $\vec{a} \times \vec{b}$, and the X axis is chosen according to the right-hand rule. Numbers in parentheses are estimated standard deviations.

In addition, the two iron atoms are displaced by 0.36 Å from the best planes through the ligand atoms O2, N1, O5, and O6 (Table V) toward the bridging oxygen atom. This results in an average Fe—OXO distance of 1.79 ± 0.01 Å which is considerably shorter than the mean of all other Fe—O bond lengths, 2.03 ± 0.01 Å. The average Fe—N bond distance is 2.25 ± 0.02 Å. These last two distances compare quite favorably with the corresponding bond lengths, Fe—O = 2.00 Å and Fe—N = 2.22 Å, found in the X-ray analysis of six-coordinate $\text{Fe}(\text{OH})_2(\text{EDTAH})$, which contains a free $\text{CH}_2\text{CO}_2\text{H}$ side chain.¹³ Not included in Table IV, but of interest, is the average dihedral angle observed between pairs of planes: O2A—FeA—OXO and N1B—FeB—OXO; N1A—FeA—OXO and O2B—FeB—OXO; O6A—FeA—OXO and O5B—FeB—OXO; O5A—FeA—OXO and O6B—FeB—OXO. This value, $146 \pm 2^\circ$, is a measure of the extent to which the two idealized octahedra are staggered across the Fe—O—Fe bond axis (a completely eclipsed structure would have a dihedral angle of 180°). Further discussion of the geometric features of the inner coordination group will be taken up later.

In Table VI we summarize all independent bond lengths and interbond angles within the HEDTA ligands. The values agree quantitatively with other crystallographic studies of similar multidentate ligands¹⁴ and appear to be independent of the coordination number of the central metal atom. The pertinent average distances are: C—N (1.48 ± 0.02 Å) and C—C (1.51 ± 0.03 Å) in the glycinate rings, C—N (1.50 ± 0.02 Å) and C—C (1.53 ± 0.03 Å) in the ethylenediamine rings, and C—O_u (1.23 ± 0.03 Å) and C—O_c (1.29 ± 0.02 Å) for the carboxylate groups, where O_u and O_c stand for uncoordinated and coordinated oxygen atoms, respectively. The difference between C—O_u and C—O_c bond lengths, while statistically unimportant, is probably chemically significant and has been observed by other workers.¹⁴ The N-hydroxyethyl

(13) J. L. Hoard, C. H. L. Kennard, and G. M. Smith, *Inorg. Chem.*, **2**, 1316 (1963).

(14) M. D. Lind, M. J. Hamor, T. A. Hamor, and J. L. Hoard, *ibid.*, **3**, 34 (1964), and references contained therein.

TABLE VI
 GEOMETRY WITHIN THE HEDTA MOIETIES^{a,b}

Bond length	Distance, Å	Bond length	Distance, Å
O1A-C1A	1.44 (3)	O1B-C1B	1.46 (2)
C1A-C2A	1.55 (3)	C1B-C2B	1.53 (3)
C2A-N1A	1.52 (2)	C2B-N1B	1.52 (2)
N1A-C3A	1.47 (2)	N1B-C3B	1.48 (2)
C3A-C4A	1.48 (3)	C3B-C4B	1.51 (3)
C4A-O3A	1.24 (2)	C4B-O3B	1.23 (2)
C4A-O2A	1.31 (2)	C4B-O2B	1.28 (2)
N1A-C5A	1.53 (3)	N1B-C5B	1.53 (2)
C5A-C6A	1.50 (3)	C5B-C6B	1.56 (3)
C6A-N2A	1.50 (3)	C6B-N2B	1.47 (3)
N2A-C7A	1.45 (3)	N2B-C7B	1.48 (2)
C7A-C8A	1.51 (3)	C7B-C8B	1.50 (3)
C8A-O4A	1.25 (3)	C8B-O4B	1.23 (3)
C8A-O5A	1.29 (3)	C8B-O5B	1.30 (2)
N2A-C9A	1.50 (2)	N2B-C9B	1.50 (2)
C9A-C10A	1.56 (3)	C9B-C10B	1.52 (3)
C10A-O6A	1.28 (2)	C10B-O6B	1.30 (2)
C10A-O7A	1.20 (2)	C10B-O7B	1.21 (2)
Interbond angle	Angle, deg	Interbond angle	Angle, deg
O1A-C1A-C2A	103 (1)	O1B-C1B-C2B	105 (1)
C1A-C2A-N1A	115 (1)	C1B-C2B-N1B	113 (1)
C2A-N1A-C3A	110 (4)	C2B-N1B-C3B	112 (1)
N1A-C3A-C4A	111 (2)	N1B-C3B-C4B	112 (1)
C3A-C4A-O3A	121 (2)	C3B-C4B-O3B	116 (2)
C3A-C4A-O2A	119 (2)	C3B-C4B-O2B	117 (1)
O3A-C4A-O2A	119 (2)	O3B-C4B-O2B	126 (2)
C4A-O2A-FeA	116 (1)	C4B-O2B-FeB	120 (1)
C3A-N1A-FeA	108 (1)	C3B-N1B-FeB	105 (1)
C2A-N1A-FeA	110 (1)	C2B-N1B-FeB	111 (1)
C5A-N1A-FeA	109 (1)	C5B-N1B-FeB	110 (1)
C3A-N1A-C5A	110 (1)	C3B-N1B-C5B	111 (1)
C2A-N1A-C5A	109 (1)	C2B-N1B-C5B	108 (1)
N1A-C5A-C6A	111 (2)	N1B-C5B-C6B	109 (1)
C5A-C6A-N2A	110 (2)	C5B-C6B-N2B	111 (1)
C6A-N2A-C7A	115 (1)	C6B-N2B-C7B	113 (1)
N2A-C7A-C8A	109 (2)	N2B-C7B-C8B	109 (2)
C7A-C8A-O4A	119 (2)	C7B-C8B-O4B	121 (2)
C7A-C8A-O5A	118 (2)	C7B-C8B-O5B	119 (2)
O4A-C8A-O5A	123 (2)	O4B-C8B-O5B	120 (2)
C8A-O5A-FeA	118 (1)	C8B-O5B-FeB	118 (1)
C7A-N2A-FeA	105 (1)	C7B-N2B-FeB	106 (1)
C6A-N2A-FeA	107 (1)	C6B-N2B-FeB	108 (1)
C9A-N2A-FeA	106 (1)	C9B-N2B-FeB	107 (1)
C6A-N2A-C9A	111 (1)	C6B-N2B-C9B	111 (1)
C7A-N2A-C9A	113 (1)	C7B-N2B-C9B	110 (1)
N2A-C9A-C10A	115 (1)	N2B-C9B-C10B	114 (2)
C9A-C10A-O7A	119 (2)	C9B-C10B-O7B	118 (2)
C9A-C10A-O6A	115 (2)	C9B-C10B-O6B	117 (2)
O7A-C10A-O6A	127 (2)	O7B-C10B-O6B	125 (2)
C10A-O6A-FeA	123 (4)	C10B-O6B-FeB	122 (1)

^a See Figure 2 for atom-labeling scheme. ^b Numbers in parentheses are estimated standard deviations.

groups are not involved in bonding to the iron atoms. Within these groups, the average C-C bond length is 1.54 ± 0.03 Å and the average C-O distance is 1.45 ± 0.02 Å. Further details may be obtained from Table VI.

The Ethylenediammonium Cation.—Of the various cations used to precipitate the [(HEDTA)FeOFe(HEDTA)]²⁻ ion from solution, only enH₂²⁺ gave crystals suitable for X-ray studies.¹ As indicated previously, it is strongly associated *via* hydrogen bonding with water molecules in the lattice. Its geometry

as determined in the present study includes a C-C distance of 1.59 ± 0.03 Å, an average C-N distance of 1.50 ± 0.03 Å, and an average angle of $108 \pm 2^\circ$ about the carbon atoms.

Qualitative Consideration of Bonding and Relation to Other M-O-M Systems

From the details of the molecular geometry of the [(HEDTA)FeOFe(HEDTA)]²⁻ complex just presented, it is possible to develop a qualitative molecular orbital description of the complex which, although crude, is relatively satisfying. The approach will be similar to that first developed by Dunitz and Orgel¹⁵ for [Cl₅RuORuCl₅]⁴⁻, where particular attention is given to π bonding within the M-O-M group.

First we assume an idealized symmetry of D_{4h} for the inner coordination group of the binuclear anion, with local C_{4v} symmetry at each Fe atom. For σ bonding, the iron atoms will use a set of orbitals which, under C_{4v} symmetry, span the representations 3A₁ + B₁ + E. This leaves orbitals of B₂ and E symmetry (commonly the d_{xy} and degenerate d_{xz}, d_{yz} orbitals) available for the five electrons of each Fe^{III} atom. Considering now the entire anion, one can combine the two sets of B₂ + E iron atomic orbitals with the filled, degenerate E_u(p_x, p_y) orbitals of the bridging O²⁻ ion to give a set of three-center π -molecular orbitals. By analogy to [Cl₅RuORuCl₅]⁴⁻, we assume the relative energies of these orbitals to be E_u < [B_{2g}B_{2u}E_g] < E_u^{*}, the orbitals in the brackets being approximately degenerate and nonbonding.¹⁵

Placing 14 electrons, five from each iron atom plus four from the oxygen atom, into these orbitals gives a ground state in which two electrons occupy the degenerate, antibonding E_u^{*} orbital. This correctly accounts for the experimentally observed¹ magnetic moment of two unpaired spins per dimer.¹⁶ The individual ($\sigma + \pi$) bond orders in the Fe-O-Fe group are 1.5, a result which is manifest in the short mean Fe-O-XO distance of 1.79 Å, compared to the mean of all other Fe-O bond lengths, 2.03 Å. The π bonding also accounts for the displacement of the iron atoms out of their local equatorial planes toward the bridging oxygen atom (Table III). Such displacements are relatively common in metal-oxygen systems characterized by extensive π bonding.¹⁷

It is instructive at this point to compare the geometry of the inner coordination group in [(HEDTA)FeOFe(HEDTA)]²⁻ with results obtained for other systems containing oxo-bridged metal atoms. The data are summarized in Table VII. Omitted from the summary are two papers by Cotton and co-workers^{18,19}

(15) J. D. Dunitz and L. E. Orgel, *J. Chem. Soc.*, 2594 (1953).

(16) Detailed measurements of the temperature dependence of the magnetic moment (μ) are in progress. It is relevant, however, that Mössbauer spectra of the dimer are identical at temperatures of 77 and 300°K, indicating the absence of any unusual magnetic behavior.

(17) See, for example, F. A. Cotton and S. J. Lippard, *Inorg. Chem.*, **5**, 416 (1966), and references contained therein.

(18) A. B. Blake, F. A. Cotton, and J. S. Wood, *J. Am. Chem. Soc.*, **86**, 3024 (1964).

(19) F. A. Cotton, S. M. Morehouse, and J. S. Wood, *Inorg. Chem.*, **3**, 1603 (1964).

TABLE VII
GEOMETRIES OF SYSTEMS CONTAINING
OXO-BRIDGED METAL ATOMS

Complex	M-O, A	M-O-M, deg	No. of π elec- trons ^a	Ref
[PyPcMn ^{III}] ₂ O ^b	1.71	178	12	3c
{[(H ₂ O)BF ₄ Fe ^{III}] ₂ O} ²⁺ c	1.8	...	14	4
{[(HEDTA)Fe ^{III}] ₂ O} ²⁻	1.79	165	14	This work
{[Cl ₅ Ru ^{IV}] ₂ O} ⁴⁻	1.80	180	12	6
{[Cl ₅ Re ^V] ₂ O} ⁴⁻	1.86	180	10	7

^a Referred to the Dunitz–Orgel molecular orbital scheme.¹⁵

^b Py = pyridine; Pc = phthalocyanato. ^c B = macrocyclic, pentadentate ligand.⁴

which describe complexes containing linear Mo–O–Mo bonds, because the presence of nonbridging oxo ligands in these compounds requires the Dunitz–Orgel molecular orbital treatment to be significantly modified.¹⁸ From the table, the M–O distances in [PyPcMn^{III}]₂O and {[(HEDTA)Fe]₂O}²⁻ are found to be 1.71 and 1.79 Å, respectively, a result which cannot be explained on the basis of the relevant covalent radii ($r_{\text{Mn(III)}} \geq r_{\text{Fe(III)}}$). A satisfactory explanation is provided by the molecular orbital treatment described above, however, since there is more π -bonding character in the M–O–M group for manganese than for iron, the latter having the . . . E_u*² configuration.

Another geometric manifestation of the difference in electronic structure between the manganese and iron dimers is the M–O–M angle, being 178° for Mn and 165° for Fe. Apparently, the lesser amount of π -bonding character in the Fe–O–Fe systems makes it more sus-

ceptible to intramolecular strains (e.g., those imposed by the chelating HEDTA ligands) and to intermolecular crystal-packing forces (Table III).

Direct comparisons of the {[(HEDTA)Fe]₂O}²⁻ structure with the remaining compounds of Table VII are not as meaningful. Of interest, however, is that, in those cases where the number of π electrons is 12 or less, the M–O–M systems retain the maximum M–O bond orders of 2 and are linear. The seven-coordinate iron complex will probably require a separate molecular orbital treatment although, from the observed Fe–O bond distance of 1.8 Å, it is likely that its electronic structure will not be too different from that of the HEDTA dimer.

Finally, we wish to emphasize that the success of the Dunitz–Orgel scheme in accounting for certain structural differences in oxo-bridged systems has been the main justification for its adoption. Clearly, there are several other electronic and steric factors present in these complexes which have not been taken into account. While more detailed calculations on these systems can (and should) be carried out, it seems likely that, in any more sophisticated treatment, extensive M–O–M π bonding will be a dominant feature.

Acknowledgments.—The authors wish to thank Professor R. Herber, Rutgers University, for obtaining and interpreting the Mössbauer spectra, Messrs. Z. Dori and E. Stiefel for useful conversations, and the Columbia University Computer Center for its cooperation. We also acknowledge the support of the National Science Foundation (Grants GP-6758 and GP-4917X).

CONTRIBUTION FROM THE DEPARTMENT OF CHEMISTRY,
FRANKLIN AND MARSHALL COLLEGE, LANCASTER, PENNSYLVANIA

A Study of the Effect of Steric Hindrance in Metal Coordination with Azo-3-pyrazolones

By FRED A. SNAVELY, DWIGHT A. SWEIGART,¹ CLAUDE H. YODER, AND ARISTIDES TERZIS¹

Received April 17, 1967

The formation constants of divalent metal ions with azo derivatives of 1-phenyl-5-methyl-3-pyrazolone have been measured in 75 vol. % dioxane. These azo derivatives are both stronger acids and stronger coordinating ligands than the analogous azo derivatives of 1-phenyl-3-methyl-5-pyrazolone. A steric effect is found with the *ortho*-substituted derivatives which decreases in the order: I > Br > Cl > F > H and C₂H₅ > CH₃. A possible explanation given is that the *ortho* groups hinder the retention of water molecules to form MCh₂·2H₂O in solution (Ch = chelate).

Introduction

Considering the wide use of the azo derivatives of 5-pyrazolones in the dye industry,² the scarcity of data on the azo derivatives of 3-pyrazolones is rather surprising. The difficulty of preparation of the latter

(1) Participants, NSF Undergraduate Research Participation Program, 1963 (A. T.) and 1966 (D. A. S.).

(2) K. Venkataramen, "The Chemistry of Synthetic Dyes," Vol. I, Academic Press Inc., New York, N. Y., 1952, pp 607–622.

probably has been the major deterrent to an extensive investigation of their properties. The commercial availability of diketene makes the preparation of 1-phenyl-5-methyl-3-pyrazolone and its azo derivatives relatively easy. We have prepared a series of azo derivatives of 1-phenyl-5-methyl-3-pyrazolone and measured their formation constants with divalent metal cations in dioxane–water solutions. It was also pos-